Effect of Wall Elasticity on the Flow Field through Stenosis Arteries and Veins

Noor Mohsin Farhan
M.Sc
farhannm@vcu.edu
University of Baghdad

Hiba N. Nashat
Physician
hnashat89@gmail.com
University of Baghdad

Najdat N. Abdullah
Professor
najdat_abdulla@ yahoo.co.uk
University of Baghdad

ABSTRACT

This paper is concerned with a numerical study of laminar pulsatile blood flow in elastic and rigid tapered arteries with tapering angles of (0,0.1, and 0.2) degrees and having stenosis of (0%, 30%, 40% and 50%) in the arterial lumen. Newtonian and non- Newtonian blood models flow through elastic artery, in addition to Newtonian blood model flow through rigid artery were considered in this study. The non-Newtonian behavior of blood was described by using cross mode for the shear thinning behavior of the blood. The flow dynamic analysis applies two-dimensional incompressible flow with Reynolds and Womersley numbers of 200 and 1.54 respectively.

Navier-stokes equations were written in form of vorticity-stream function and solved by a finite difference technique with necessary initial and boundary conditions in concert with the biophysical point of view using FORTRAN 90 program. The comparisons between the results considering rigid and elastic arteries showed a decrease in wall shear stress and reduce in pressure drop and less extended separation regions for the elastic artery. The deformation of the arterial wall cannot be neglected while dealing with blood flow studies. The comparison results for the non-Newtonian and the Newtonian fluid flows showed that, the non-Newtonian effects weakness in distortion of flow pattern, pressure drop distribution and wall shear stress. Also, the numerical results were compared with previous researches results.

Key words: simulation, elastic wall, non-Newtonian fluid, pulsatile flow, stenosis, coronary artery; blood flow.

INTRODUCTION

Partial narrowing of arteries, commonly referred to as stenotic obstruction, arising from the deposition of fatty substances in the arterial lumen, is one of the most frequent anomalies in blood circulation leading to the atherosclerosis, a common arterial disease which severely affects human health. The disease is particularly dangerous in the coronary artery and will reduce the blood supply to the heart muscle. In Iraq; partially, in Ibn al-Nafees hospital, it was found that around 10000 patients suffered from atherosclerosis of coronary artery every year. There has been a great interest in past years from many investigators to study blood flow in stenotic arteries to obtain useful information which may lead to early detection, prevention and diagnosis of various cardiovascular diseases under different cases such as rigid or elastic vessel, Newtonian or non-Newtonian fluid, and or unsteady flow.

The blood dynamics in the early stages of the atherosclerotic process was investigated theoretically by **Cavalcanti, 1995**. The mode incorporates: Newtonian fluid, elastic wall motion,

and unsteady flow. The results indicated that, the shape of velocity distributions is strongly perturbed by the stenosis. Comparison between Newtonian and three models of non-Newtonian fluid was studied by **Tu and Deville, 1996**. The geometry corresponds to a rigid tube with a partial occlusion. Computations results showed that, the viscosity of blood could significantly affect the flow phenomena.

An experimental work of the post-stenotic velocity flow field corresponding to different flow waveforms was done by **Siouffi et al., 1998** through rigid vessel. He recognized that, beyond the influence of the flow parameters such as the Reynolds number and the frequency parameter, velocity profiles highly depended on the flow waveform. **Pedrizzetti et al., 2002**, studied pulsatile flow inside an elastic artery to understand the influence of elasticity in artery flow for Newtonian fluid. The results showed that, during the acceleration, the synchronous deformation of the wall leads to a less extended separated region while the contraction of the vessel during the deceleration phase of the imposed pulse tends to diminish the value of the negative tangential stress. **Tang et al., 2003** investigated experimentally and numerically the effect of asymmetry stenosis in elastic thick wall under pulsation condition of flow. The results indicated that, asymmetry stenosis led to a large flow separation region, high shear stress and high artery compression. Study of the axial and radial displacement of a thick elastic wall was carried out by **Moayeri and Zendehbudi, 2003**. The results showed that, the axial wall displacements were smaller than the radial displacements due to initial axial tension of the wall and tethering action of the surrounding tissues. The variations of the dimensionless radial stress across the wall thickness were smaller than the variations of the dimensionless circumferential stress over the wall thickness at same time. The effect of tapering angle with stenosis existence inside rigid artery was studied by **Liu et al., 2004**. A comparison of the tapering effect on the wall shear stress, WSS, revealed that, the tapering of the artery did not change the flow pattern, but only changed the values. The peak value of the wall shear stress for the tapered artery was higher than that without tapering. In the human right coronary artery, comparison the effects of different blood viscosity models (Newtonian and non-Newtonian) on the WSS distributions was investigated by **Johnston et al., 2006**. The comparison would allow assessing whether or not it is necessary to include non-Newtonian blood models in modelling blood flow. Assuming that, the flow was pulsatile and the artery wall was rigid. They conclude that, the flow within the human right coronary artery in great detail, a non-Newtonian model was more appropriate. **Mandal et al., 2007,** studied the pulsatile flow of blood under the influence of externally imposed periodic body acceleration through a stenosed elastic artery. Results showed that all the instantaneous flow characteristics were affected by the application of body acceleration. Serious physiological problems, viz. the occurrence of back flow and vanishing of WSS could be caused by body acceleration. Effect of magnetic field on the behaviour of blood flow through artery was investigated by **Misra and Shit, 2007**. Since blood consists of a suspension of red blood cells containing hemoglobin which contains iron oxide and it was quite apparent that, blood was electrically conducting. Numerical model was used that represent Newtonian blood flow through elastic artery in the presence of transverse magnetic field under the action of pulsatile pressure gradient. The study showed that, in the case of aorta and femoral arteries the magnetic field intensity brings about great changes in the axial velocity of blood. The changes were relatively small in the case of coronary artery, this change was decreasing in velocity with an increase in magnetic field strength. The wall shear stress,WSS reduced with increased in the value of magnetic parameter.

Three dimensions pulsatile blood flow through a rigid model of the carotid artery bifurcation was simulated by **Nguyen et al., 2008**. It was found that the bifurcation angle affect the formation of low stress regions on the carotid walls. The main conclusions were: larger carotid artery angles generally increase the area of blood recirculation and lower the WSS value on the sinus wall, hence increasing the risk of plaque build-up. Symmetric bifurcations were found to increase the WSS on the sinus wall and ease the risk of vascular disease. Curved pipes with different curvatures and bifurcating pipes with different branching angles were investigated by **Chaniotis et al., 2010** via numerical simulation. WSS distributions were presented for pulsatile and non-Newtonian blood flow conditions. Specific preferential sites of an average low WSS were found at the outer regions of the bifurcating branches just after the bifurcation, and at the outer-entry and inner-exit flow regions of the curved vessel segment.

Devajyoti and Moumita ,2013, developed a mathematical model to study the steady flow of blood (Newtonian fluid) through an inclined tapered constricted artery with an axial slip in velocity at the tapered vessel wall. The present model was intended to investigate the combined influence of tapering angle, slip at wall, inclined artery, Newtonian nature and non-symmetrical stenosis, for blood flow through constricted arteries. Analytic expressions for impedance to flow and wall shear stress were obtained and their variations with several flow parameters were presented graphically. **Syeda, et al., 2013**, carried out numerical analysis to demonstrate the variation of two hemodynamic forces: wall shear stress and pressure in the flow field of stenotic and rigid artery. The artery has 75% stenosis severity with axisymmetric cosine shaped stenosis. A sinusoidal pulsatile flow was assumed as inlet boundary condition. During the simulation both standard kω model of low Reynolds correction and standard kε model were used. Some analysis showed better agreement with previous experimental results. The peak wall shear stress was found to be located proximal to the stenosis throat. The results illustrated oscillating wall shear stress downstream the stenosis throat throughout the time period. The pressure gradient at the throat was highest at peak flow condition. **Titus and Balázs , 2014**, Simulated blood flow in large blood arteries, taking into consideration the non-Newtonian character of the blood together with the viscoelastic behavior of the arteries wall. The simulation was performed with different pathological cases, blood artery had a stenosis or an aneurysm. The numerical simulations were made by using the COMSOL Multiphysics 3.3 package. A real case of a stenosis artery was considered. The velocity field, at a certain time (t=8s) was presented. Comparison showed that the result obtained numerically coincides well with those got by laboratory measurement. **Mekheimer, et al., 2015**, they analyzed blood flow through inclined catheterized arteries having a balloon with time-variant overlapping stenosis The nature of blood in small arteries were analyzed mathematically by considering it as a Carreau fluid. The analysis was carried out for an artery with a mild stenosis. The problem was formulated using a perturbation expansion in terms of a variant of the Weissenberg number to obtain explicit forms for the axial velocity, the stream function, the pressure gradient, the resistance impedance and the wall shear stress distributions. The results for various values of the physical parameters were obtained and showed that the stream lines had a clearly distinguished shifting towards the stenotic region and this shifting appears near the wall of the balloon, while they had almost disappeared near the stenotic wall.

Summary of the past studies indicated that, no work had been published on the subject of non-Newtonian fluid flow though elastic constricted taper artery with stenosis under pulsation condition. Therefore, the present study considers the flow of Newtonian and non-Newtonian fluids through elastic constricted taper artery under pulsation condition and percent of stenosis to

investigate the effects of wall deformability, non-Newtonian viscosity, stenosis percent and the tapering angle on the blood flow parameters through coronary artery.

MATHEMATICAL MODELING

The considered geometries in this study are taken as approximate shapes from CT scan images of human arteries of almost (300) visiting suffering patients in Ibn al-Nafees hospital in Baghdad over a year of study. For more accurate and realistic modeling artery, walls of arteries are considered to be elastic. The thickness of the wall was not showing in CT scan, therefore, a thickness for both geometries is assumed uniform and equal to the typical value of 1 mm for the abdominal aorta, **Fung,1986.** Three cases are considered, (case 1): a Newtonian fluid model with a rigid wall assumption, Case (2): a Newtonian fluid model with an elastic wall assumption and Case (3): a non- Newtonian fluid model with an elastic wall assumption.

The tapered vessel segment having an axially symmetric stenosis is mathematically modeled as an elastic tube with a circular section. The geometry of the stenotic arterial segment is shown schematically in **Fig.1** and is described mathematically as follows: **Mandal, 2005.**
At the stenosis region:

$$\mathrm{R}=\left[(m\mathrm{x}+a)-\frac{\tau_m \sec\theta(\mathrm{x}-l_o)}{\tau_m^2 \sin\theta^2-\frac{l_s^2}{4}}\{l_s-(\mathrm{x}-l_o)\}\right]a_1(\mathrm{t})$$

Otherwise, at the regions without stenosis:

$$R=(m\mathrm{x}+a)a_1(\mathrm{t}) \qquad (1)$$

where R denotes the radius of the tapered arterial segment as a function of both time (t) and axial direction (x), due to vessel deformability and stenosis, respectively. a is the constant undisturbed inlet radius, θ , is the angle of converging tapering $(\theta<0)$, l_s, is the length of the stenosis, l_o, is the location of the stenosis and $\tau_m \sec\theta$ is taken to be the critical height of the stenosis for the tapered artery appearing at $\mathrm{x}=l_o+\frac{l_s}{2}+\tau_m \sin\theta$ and $m=\tan\theta$ represents the slope of the tapered vessel. The time-variant parameter $a_1(t)$ is given by:

$$a_1(\mathrm{t})=1-b(\cos c\mathrm{t}-1)e^{-bc\mathrm{t}} \qquad (2)$$

in which c represents the angular frequency and equals to $2\pi f$, f being the heart pulse frequency and b is a constant. The arterial segment is taken to be of finite length L, as shown in **Fig.1**.

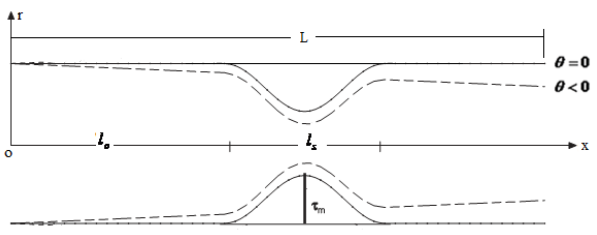


Figure 1. Schematic diagram of the tapered artery with stonsis.

Consider the blood flow in the arterial segment to be pulsating, axisymmetric, two-dimensional and laminar flow. The continuity and Navier-Stokes equations in radial and axial directions (r, x), which govern the blood flow are written in the cylindrical coordinates as, **Pontrelli, 1999.**

$$\frac{\partial \mathrm{u}}{\partial \mathrm{x}} + \frac{\partial \mathrm{v}}{\partial \mathrm{r}} + \frac{\mathrm{v}}{\mathrm{r}} = 0 \tag{3}$$

$$\rho\left(\frac{\partial \mathrm{v}}{\partial \mathrm{t}} + \mathrm{u}\frac{\partial \mathrm{v}}{\partial \mathrm{x}} + \mathrm{v}\frac{\partial \mathrm{v}}{\partial \mathrm{r}}\right) = -\frac{\partial \mathrm{p}}{\partial \mathrm{r}} + \mu\left(\frac{\partial^2 \mathrm{v}}{\partial \mathrm{x}^2} + \frac{\partial^2 \mathrm{v}}{\partial \mathrm{r}^2} + \frac{1}{r}\frac{\partial \mathrm{v}}{\partial \mathrm{r}} - \frac{\mathrm{v}}{\mathrm{r}^2}\right) + \frac{\partial \mu}{\partial \mathrm{x}}\left(\frac{\partial \mathrm{v}}{\partial \mathrm{x}} + \frac{\partial \mathrm{u}}{\partial \mathrm{r}}\right) + 2\frac{\partial \mu}{\partial \mathrm{r}}\frac{\partial \mathrm{v}}{\partial \mathrm{r}} \tag{4}$$

$$\rho\left(\frac{\partial \mathrm{u}}{\partial \mathrm{t}} + \mathrm{u}\frac{\partial \mathrm{u}}{\partial \mathrm{x}} + \mathrm{v}\frac{\partial \mathrm{u}}{\partial \mathrm{r}}\right) = -\frac{\partial \mathrm{p}}{\partial \mathrm{x}} + 2\frac{\partial \mu}{\partial \mathrm{x}}\frac{\partial \mathrm{u}}{\partial \mathrm{x}} + \frac{\partial \mu}{\partial \mathrm{r}}\left(\frac{\partial \mathrm{v}}{\partial \mathrm{x}} + \frac{\partial \mathrm{u}}{\partial \mathrm{r}}\right) + \mu\left(\frac{\partial^2 \mathrm{u}}{\partial \mathrm{x}^2} + \frac{\partial^2 \mathrm{u}}{\partial \mathrm{r}^2} + \frac{1}{\mathrm{r}}\frac{\partial \mathrm{u}}{\partial \mathrm{r}}\right) \tag{5}$$

where t is time, ρ is the constant blood density and $\mathrm{p} = \mathrm{p}(\mathrm{x}, \mathrm{t})$ is the pressure; $\mathrm{v} = \mathrm{v}(\mathrm{r}, \mathrm{x}, \mathrm{t})$ and $\mathrm{u} = \mathrm{u}(\mathrm{r}, \mathrm{x}, \mathrm{t})$ are the components of velocity in the radial (r) and the axial (x) directions respectively.

In the present study, the shear thinning behavior of blood viscosity is simulated by the cross model, where the apparent viscosity is expressed as a function of the shear rate **,Javadzadegan et al., 2009**, as follows:

$$\mu(\dot{\gamma}) = \mu_\infty + \frac{\mu_0 - \mu_\infty}{1 + (\Lambda\dot{\gamma})^{1-k}} \tag{6}$$

Where the constants μ_0 and μ_∞ are the asymptotic viscosities at zero and infinity shear rate respectively.

$\dot{\gamma}$ shear rate is given for the case of two-dimension motion by **Mandal et al., 2007**:

$$\dot{\gamma} = \left[2\left(\frac{\partial \mathrm{u}}{\partial \mathrm{x}}\right)^2 + \left(\frac{\partial \mathrm{u}}{\partial \mathrm{r}} + \frac{\partial \mathrm{v}}{\partial \mathrm{x}}\right)^2 + 2\left(\frac{\partial \mathrm{v}}{\partial \mathrm{r}}\right)^2 + 2\left(\frac{\mathrm{v}}{\mathrm{r}}\right)^2\right]^{\frac{1}{2}} \tag{7}$$

k is the power index and $\Lambda \geq 0$ in unit of time representing the degree of shear-thinning.

Introduce the following dimensionless variables: **Moayeri and Zendehbudi, 2003**, and **Pedrizzetti, et al., 2002.**

$$r=\frac{\mathrm{r}}{a},\quad x=\frac{\mathrm{x}}{a},\quad t=\mathrm{t}*f,\quad u=\frac{\mathrm{u}}{U},\quad v=\frac{\mathrm{v}}{U},\quad p=\frac{\mathrm{p}}{\rho U^2},\quad \dot{X}=\frac{\mu}{\mu_\infty},\ \text{and}\ \delta=\frac{\mu_0}{\mu_\infty} \tag{8}$$

where U is the maximum average velocity over a. For convenience in solving the governing equations, the stream function-vorticity form of the equation is adopted. This form has a major advantage over the primitive variable form in two-dimensional incompressible flow, as it satisfies the equation of continuity automatically. Introduce the dimensionless stream function ψ and the dimensionless vorticity ω by **Liu et al., 2004.**

$$u=\frac{1}{r}\frac{\partial\psi}{\partial r}\qquad,\qquad v=-\frac{1}{r}\frac{\partial\psi}{\partial x}$$

$$\text{and}\quad \omega=\frac{\partial v}{\partial x}-\frac{\partial u}{\partial r} \tag{9}$$

Eliminating p from Eqs. (4) and (5) and using Eqs. (8) and (9) to get vorticity-transport equation, **Pontrelli, 1999**, and Poisson equation as shown bellow, **Pedrizzetti et al., 2002**:

$$\frac{\lambda^2}{\mathrm{Re}}\frac{\partial\omega}{\partial t}+\frac{1}{r}\frac{\partial\psi}{\partial r}\frac{\partial\omega}{\partial x}-\frac{1}{r}\frac{\partial\psi}{\partial x}\frac{\partial\omega}{\partial r}+\frac{\omega}{r^2}\frac{\partial\psi}{\partial x}=\frac{1}{\mathrm{Re}}\left(\frac{\partial\dot{X}}{\partial x}\cdot 2\frac{\partial\omega}{\partial x}+\dot{X}\left(\frac{\partial^2\omega}{\partial x^2}+\frac{\partial^2\omega}{\partial r^2}+\frac{1}{r}\frac{\partial\omega}{\partial r}-\frac{\omega}{r^2}\right)+\left(\frac{\partial^2\dot{X}}{\partial x^2}-\frac{\partial^2\dot{X}}{\partial r^2}\right)*\left(\frac{1}{r}\frac{\partial^2\psi}{\partial r^2}-\frac{1}{r}\frac{\partial^2\psi}{\partial x^2}-\frac{1}{r^2}\frac{\partial\psi}{\partial r}\right)+\frac{\partial\dot{X}}{\partial r}\left(2\frac{\partial\omega}{\partial r}+\frac{\omega}{r}\right)+2\frac{\partial^2\dot{X}}{\partial x\partial r}\left(\frac{1}{r^2}\frac{\partial\psi}{\partial x}-\frac{2}{r}\frac{\partial^2\psi}{\partial x\partial r}\right)\right) \tag{10}$$

$$\frac{\partial^2\psi}{\partial x^2}+\frac{\partial^2\psi}{\partial r^2}-\frac{1}{r}\frac{\partial\psi}{\partial r}=-\omega r \tag{11}$$

where Re is the Reynolds number , $\mathrm{Re}=\frac{\rho U a}{\mu_\infty}$, and λ is the Womersley number**,** $\lambda=a\sqrt{\frac{2\pi f\rho}{\mu_\infty}}$ **.**

BOUNDARY AND INITIAL CONDITIONS

a- On the symmetry axis: **Chakravarty and Sen, 2008.**

$$\psi\big|_{r=0}=0 \tag{12}$$

$$\omega\big|_{r=0}=0 \tag{13}$$

b- At the elastic wall, the flow velocity must be equal to the material wall velocity, **Pedrizzetti et al., 2002** and **Mandal, 2005**:

$$\psi\big|_{r=R} = 0.25(1+\sin 2\pi \frac{t}{T}) \tag{14}$$

$$\omega\big|_{r=R} = \frac{1}{R}\left(R.\frac{\partial^2 R}{\partial x \partial t} - \frac{2}{\Delta r^2}\left(\psi\big|_{r=R-\Delta r} - \psi\big|_{r=R}\right)\right) \tag{15}$$

c- At the inlet cross section, the flow is assumed to be fully developed, **Chakravarty and Sen, 2008**:

$$\frac{\partial \psi}{\partial x} = \frac{\partial \omega}{\partial x} = 0 \tag{16}$$

d- At the outlet cross section, fully developed flow has been assumed.

$$\frac{\partial \psi}{\partial x} = \frac{\partial \omega}{\partial x} = 0 \tag{17}$$

2- The initial conditions:

There is a flow takes place when the system is at rest (t=0), **Chakravarty and Sen, 2008:**

$$\omega = \psi = 0.001 \tag{18}$$

The governing equations, Eqs. (10) and (11), which are subjected to the boundary and initial conditions, of Eqs.(12) to (18) are solved by using the finite difference method. To perform a careful parameters analysis, streamline, wall shear stress, and axial velocity profile results are plotted and discussed in following subsection during cycle of pulsation flow. The results are chosen at different time steps as shown in **Fig.2**.

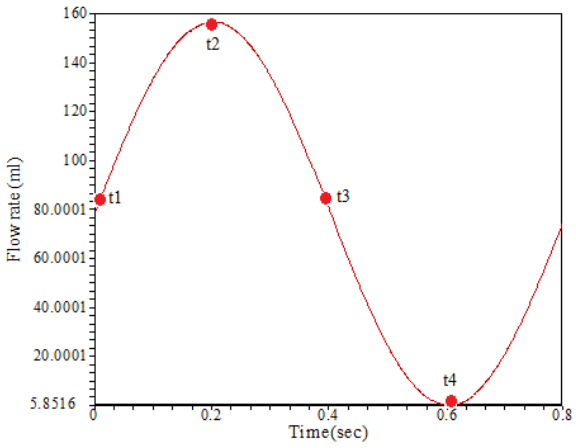


Figure 2. Blood flow rate behavior at one heart beat.

The analysis is based on four time steps at one heart beat and considered as a key points during the period, and are as follows:

- t1= 0.01s is near the beginning of the cycle.
- t2=0.2s is the point of maximum flow rate.
- t3=0.4s is time of maximum radius.
- t4=0.6s is the point of minimum flow rate.

RESULTS AND DISCUSSIONS

The problem considered is unsteady laminar flow through a constricted coronary artery. During the computational procedure, the characteristic parameters: a, L, l_o, & l_s = 0.8, 50, 20, and 16mm respectively. ρ = $1060\,kg/m^3$, μ_∞ = $0.00345\,Ns/m^2$, μ_0 = $0.056\,Ns/m^2$, $k = 0.285$, $\Lambda = 1.007s$, and T = 0.8s were used with Re = 200, and λ = 1.54. The computed results checked for convergence with an accuracy degree of (10^{-5}) when the time-steps is chosen to be $\Delta t = 0.0001$ sec and the number of grid points along the axis in (x, r) were (150, 36) respectively.

To investigate the effect of wall elasticity on the blood flow performance, three cases are considered:

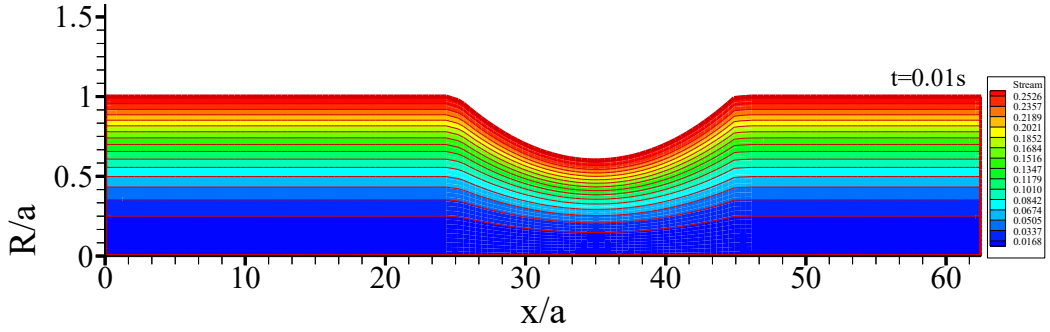
Case 1: a Newtonian fluid model with a rigid wall assumption.
Case 2: a Newtonian fluid model with an elastic wall assumption.
Case 3: a non- Newtonian fluid model with an elastic wall assumption.

1. Effects of Artery Wall Elasticity on Flow Field

To study the effects of wall elasticity, comparison between (case1) and (case 2) results will be done, at the same inlet flow rate with 40% stenosis and at four time steps. The results of wall elasticity on instantaneous streamline pattern for rigid and elastic, dimensionless axial velocity profiles and wall shear stress for both rigid and elastic walls are shown in **Figs. 3, 4, 5 and 6** respectively.

a. Instantaneous streamline pattern

- For rigid wall



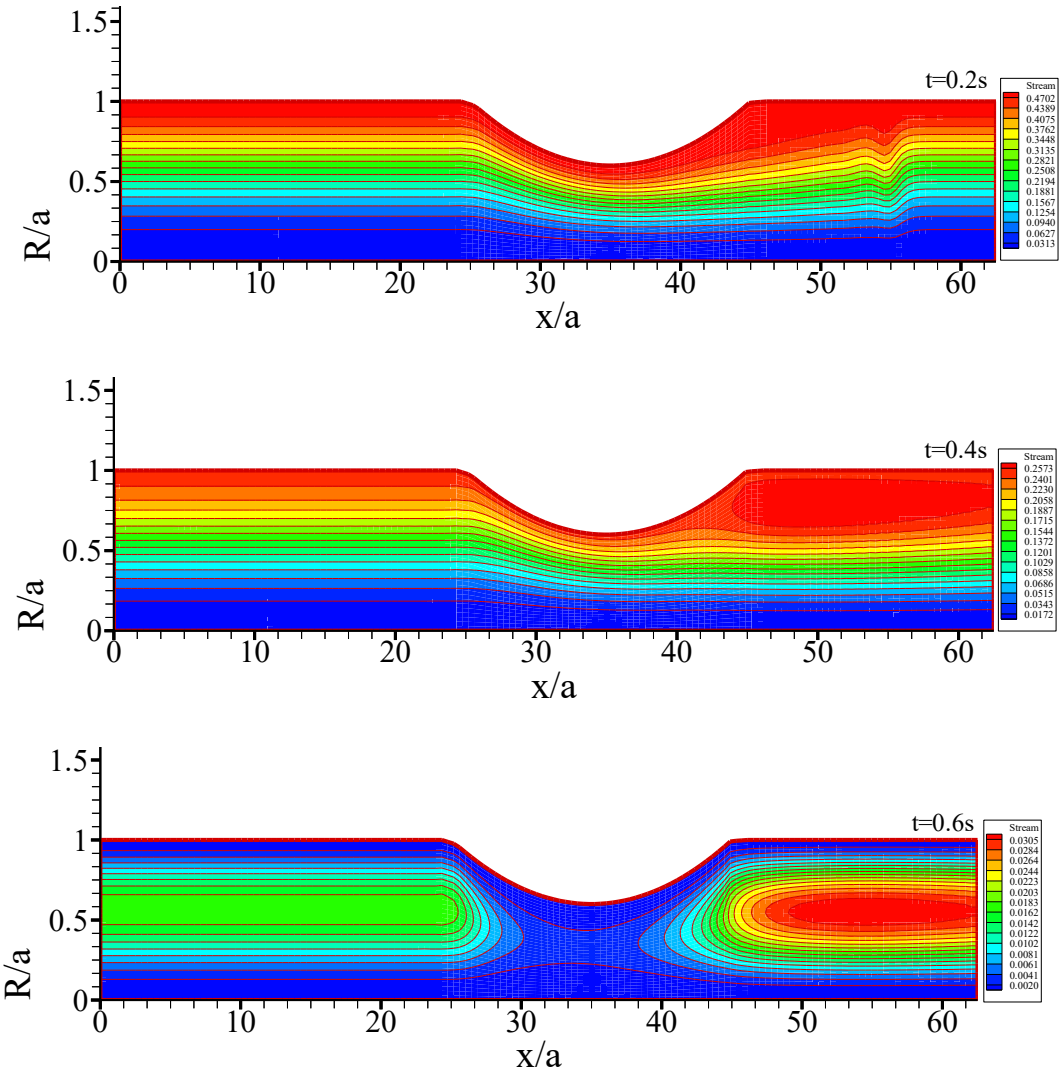


Figure 3. Instantaneous streamline pattern at different time steps in pulsatile flow inside rigid artery.

- For elastic wall

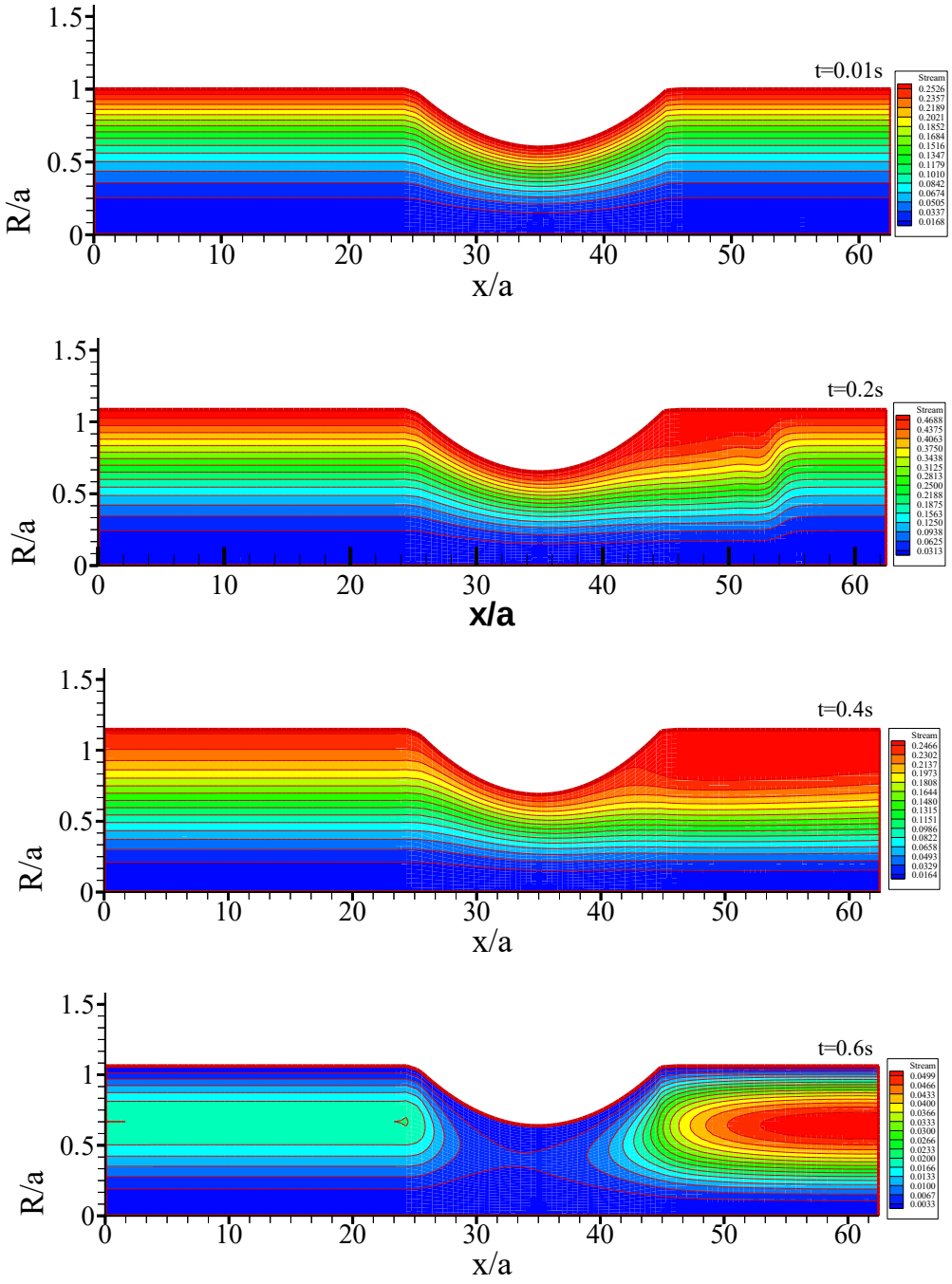


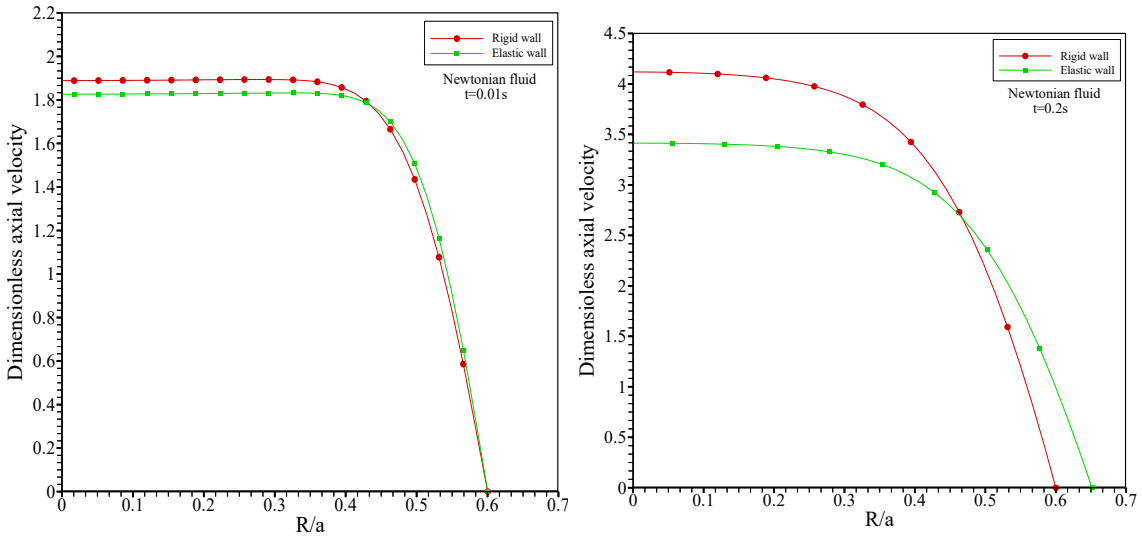
Figure 4. Instantaneous streamline pattern at different time steps in pulsatile flow inside elastic artery.

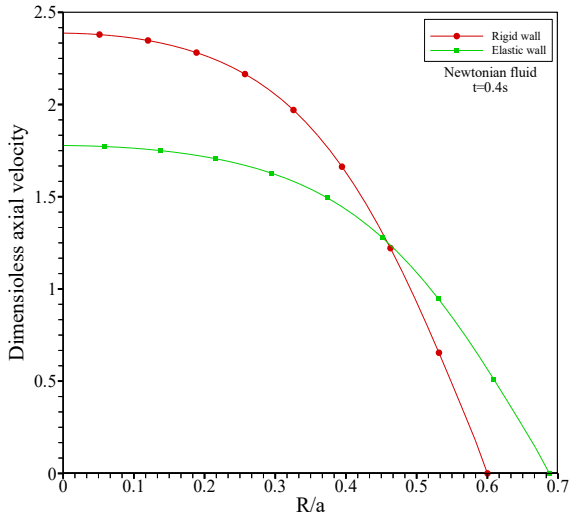
The flow dynamic must be preliminarily analyzed in the rigid artery case, this is shown in **Fig.3** at four instants during one period and the flow fields for the elastic case is shown in **Fig.4** at the same instants of the rigid case, to visualise the wall deformation effect. The results indicated that, the stream line changes as inlet flow rate changes according to **Fig.2**. In general, the results at the selected time steps of two figures indicated that, at t=0.2s which represents a

point of maximum flow rate, the separation region is great after the stenosis and continues in growing until reaches the time t=0.6s since became the separation after and before the stenosis.

Particularly, at the elastic wall case, **Fig.4**, during the cycle, the synchronous deformation of the wall leads to a less extended separated region. Same trends are observed by **Pedrizzetti et al., 2002**.

b. Dimensionless axial velocity profiles





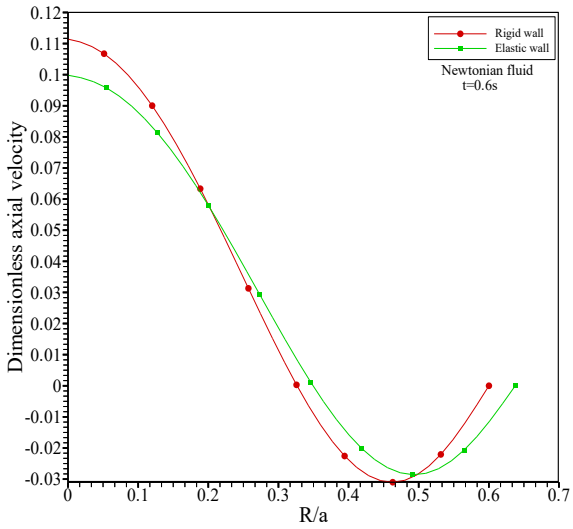
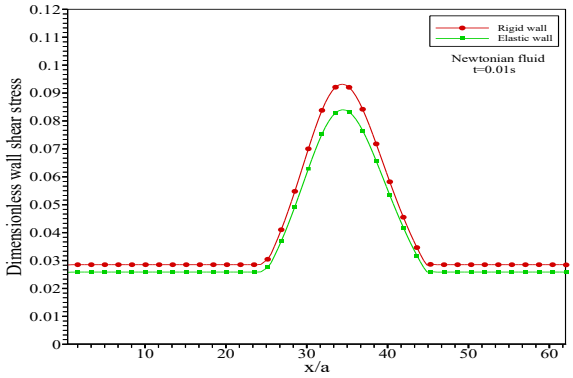


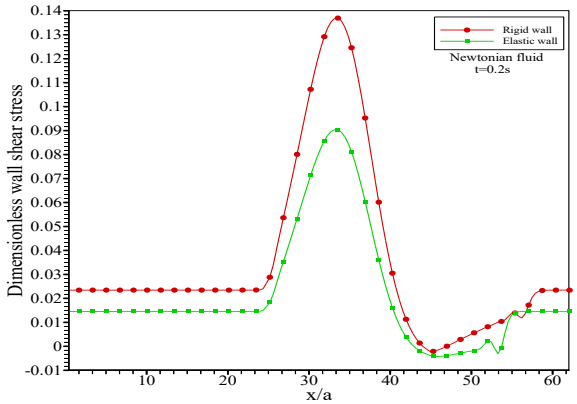
Figure 5. Variation in axial velocity of flow.

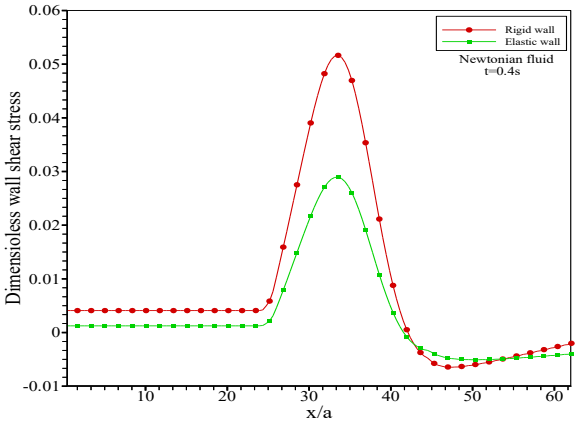
Fig.5 shows the variation in dimensionless axial velocity of the rigid and compliant wall models at different times of the cycle. The velocity presented is evaluated at the critical height of the stenosis. The results showed that, at all time steps, the curves are all featured to decrease from their individual maxima at the axis as one move away from it and finally drop to zero on the wall surface. The axial velocity profile of elastic wall is found to be wider and more blunted in the center that because the radius expansion. Near the axis, the axial velocity of elastic wall model is smaller than rigid wall at all selected time steps and reduces the maximum velocity at the throat at all the times, hence causes to pressure drop more than rigid wall case. This can be explained that; the pressure exerted on the wall by the fluid will push the wall outward causing expanding the flow area, which in return will change the velocity profiles. The flow separation indicated by negative velocity region near the wall. The reverse flow zone tended to be at t=0.6sec at the throat that chosen as a test position, but at the other time steps no recirculation was observed for the same position. Therefore, the figures show the important of wall elasticity in dealing with flow in arteries.

c. Variation in dimensionless wall shear stress

The dimensionless wall shear stress (WSS) is the representation of the magnitude and rate of change of blood flow close to the artery wall and has been linked to the pathogenesis of atherosclerosis. WSS mapping should become part of the important approach to early detection of atherosclerosis.


Rigid wall
Elastic wall
Newtonian fluid
t=0.01s
Dimensionless wall shear stress
x/a


Rigid wall
Elastic wall
Newtonian fluid
t=0.2s
Dimensionless wall shear stress
x/a


Rigid wall
Elastic wall
Newtonian fluid
t=0.4s
Dimensioless wall shear stress
x/a

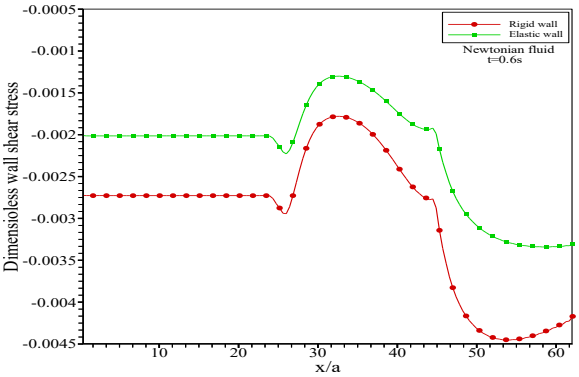

Rigid wall
Elastic wall
Newtonian fluid
t=0.6s
Dimensioless wall shear stress
x/a

Figure 6. Comparison of dimensionless wall shear stress,WSS, between rigid and elastic walls at different time steps.

Fig.6 shows comparison of the numerical results for the WSS distribution along the straight artery wall of two cases (case1 and case2) at t = 0.01, 0.2, 0.4, and 0.6s. When the flow begins to accelerate (at t = 0.01s), the WSS increases to a maximum positive value at the throat of the stenosis. It is observed that the WSS changes in direction in the downstream vicinity of the throat, that is, the corresponding values change to low negative values. At the peak flow time (i.e. t= 0.2s), the maximum positive value reaches its peak value and the flow separation region grows. At time t = 0.4s, the maximum positive value decreases and the flow separation region continues growing. Until time t= 0.6s (minimum inlet flow rate), the WS is oscillating and negative everywhere in the computational region near the wall. As the blood flow is further reduced until reaching minimum flow, the backward flow gradually occupies the whole blood vessel. It is noticed that the WSS upstream of the stenosis isn't disturbed at these times. It is obvious from the figures that the maximum WSS for the elastic wall case is less than that for rigid wall case.

2. Effects of Non-Newtonian Property of Fluid on Flow Field

Non-Newtonian fluid flow in a stenosed coronary artery is investigated numerically by using the cross model for the shear thinning behavior of the blood. To study the effects of non-Newtonian property of fluid on flow field, comparison between (case2) and (case 3) results for wall shear stress are performed, at the same inlet flow rate and elastic wall assumption with 40% stenosis.

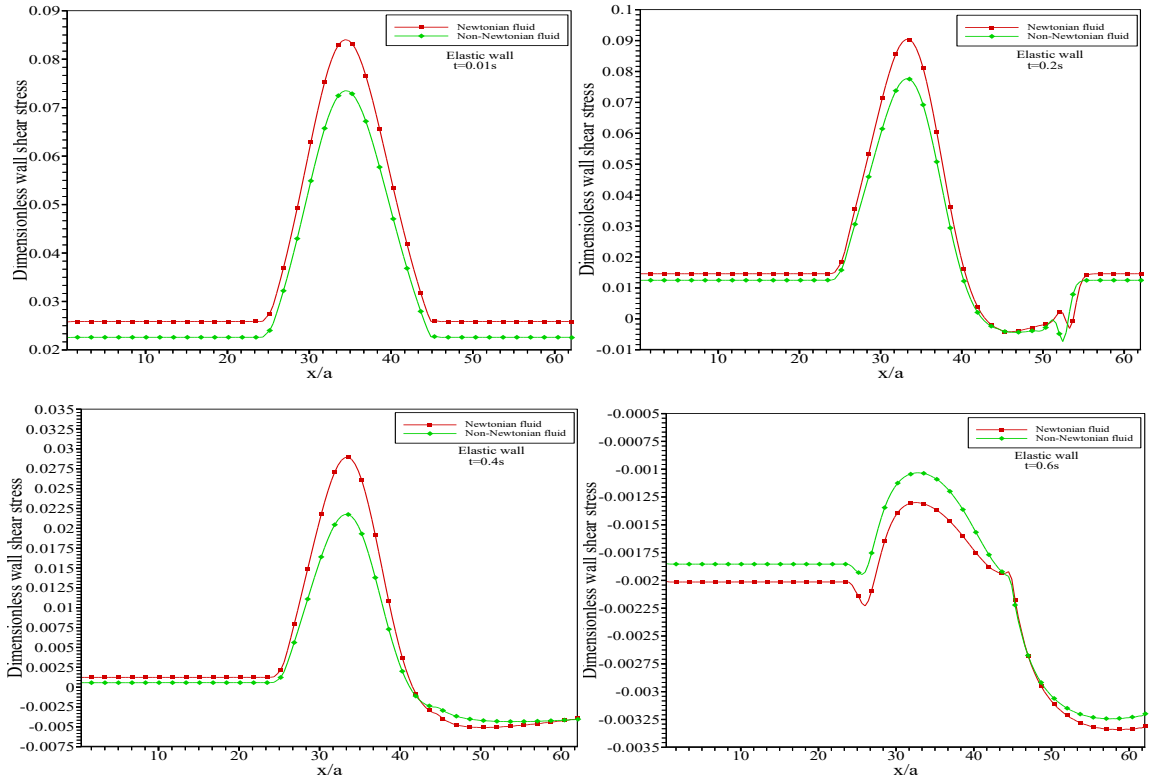


Figure 7. Comparison of WSS between Newtonian and non-Newtonian fluids.

Fig.7 shows the behavior of the WSS distributed over straight elastic arterial segments with 40% stenosis for the different time steps and also their responses to the blood viscosity. The differences in WSS between the Newtonian and non-Newtonian models are more visible. The WSS peak value of a Newtonian fluid is greater than the value of a non-Newtonian fluid at all time steps, this agrees with the results of, **Chen, 2006**. In general, during the accelerating phase of systole, the WSS value rises sharply at the minimum cross section area and then decreases quickly reversing its direction at the distal of the stenosis. It also reaches a maximum rising value at t=0.2s. But at t=0.01s, it records maximum WSS values before the stenosis. It should also be noticed that there is a region just distal to the stenosis where shear stress becomes negative. This direction change of the shear stress is due to flow separation and recirculation in that region. At the midpoint of diastolic phase, t=0.6s, the WSS values is negative everywhere in the blood artery because the backward flow occur along the blood artery.

3. Effect of Stenosis Percentage on Flow Field

Stenosis severity is one of the most important factors affecting the flow. The effect of (0, 30, 40, and 50) % stenosis on WSS distribution of the same inlet flow rate was studied for case3, as follows:

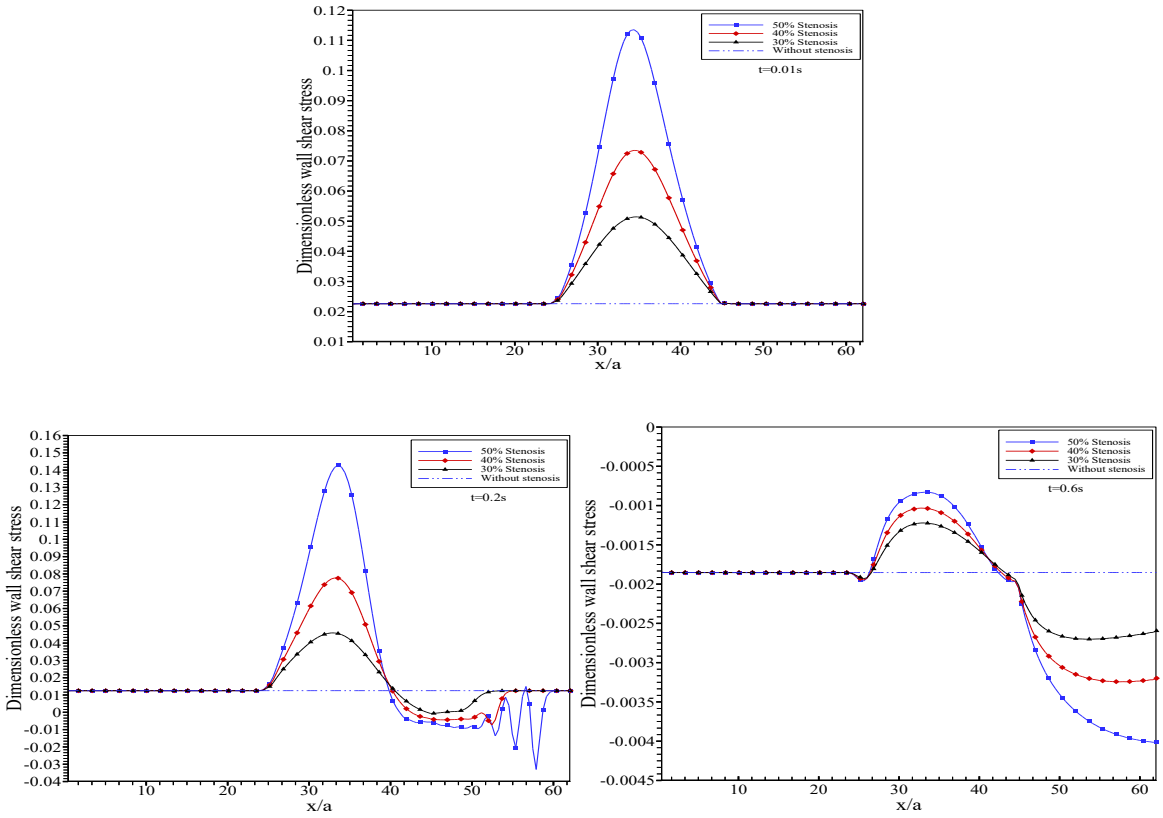


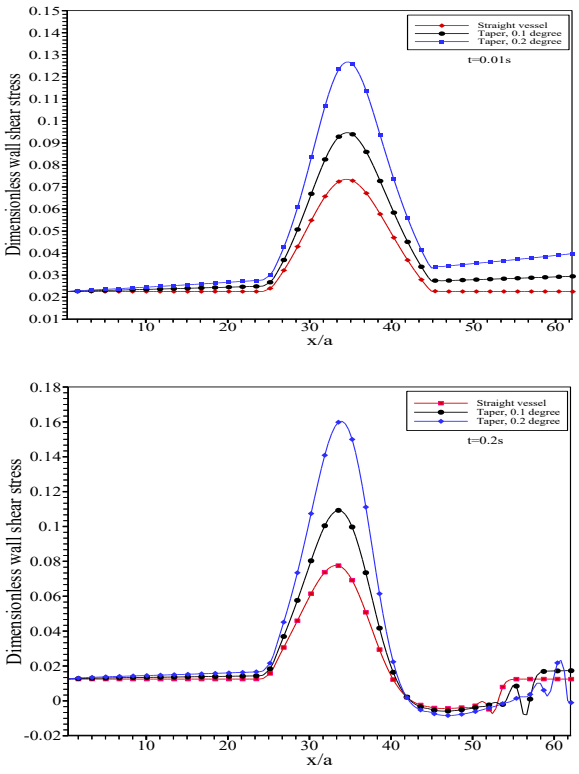
Figure 8. Effect of stenosis severity on the WSS distribution at different time steps.

Fig.8 shows the effect of stenosis percentages on WSS distribution of non-Newtonian fluid along the axial distance of elastic straight artery. It indicates that, comparison of the

distributions of the WSS at different stenosis percent reveals that, the height of stenosis has a strong influence on the WSS at the throat and downstream of the throat, and on the length of the flow separation region. WSS value increases with increasing stenosis percentage at the throat and the downstream of throat. Since high WSS at the throat will damage the artery wall, the WSS at the throat deserves to be noticed. Considering that the flow separation region may prolong the residence time of the particles in the blood, the region may allow the phenomenon of lipid deposition and cell leading in-turn to atherosclerosis. Hence the post-stenotic zone could be prone to the propagation of all subsequent complications including hypoxia and infarction in severe cases. The WSS upstream of the stenosis doesn't disturb at any time, whether the stenosis exists or not. These results agree with results of, **Liu, 2004.**

4. Effect of Tapering Angle on Flow Field

One of the simplifying assumptions in this study and some previous studies is that the artery is without branches. Real blood arteries are often variable cross section. The non-uniform cross-sectional area is associated with branching. The taper is generally very mild, and it is possible to evaluate branches effect approximately without extensive calculations, **Fung, 1997**. The effect of tapering with 0.1° and 0.2° tapering angles for the same inlet flow rate was studied for case3 at 40% stenosis, as follows:



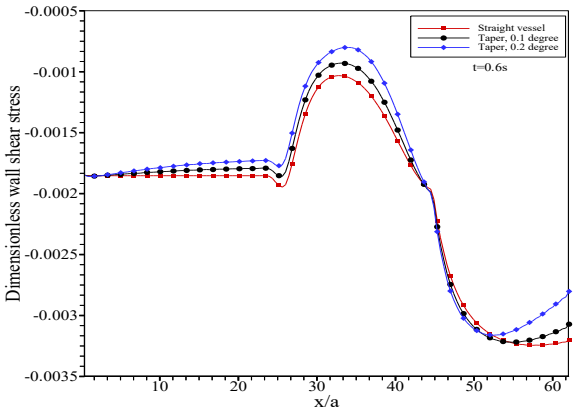


Figure 9. Comparison of WSS between different tapering angles at different time steps.

Fig.9 shows that the WSS distribution of non-Newtonian fluid along axial length of elastic artery at different tapering angles (0°, 0.1° and 0.2°), with 40% stenosis. It indicates that, the WSS value increases with increasing distance into tapered section; this because of the taper artery that leads to increase the velocity as diameter decreases. The values of WSS at 0.2° tapering are higher than that at 0.1° tapering. Also, the WSS distributions indicate same behavior at different tapering angles but increasing in its values along axial length was observed with increase in tapering angle. Due to the tapering, the oscillation amplitude of the WSS is higher than that of a non-tapered artery.

CONCLUSIONS

In this paper, the unsteady flow inside an elastic and rigid artery with a circular cross section varying along the tube axis has been studied. The problem has been analyzed by the numerical solution of the Navier–Stokes equations, in the vorticity-stream function formulation, assuming axial symmetry under laminar flow condition. A shear thinning behavior was used to express blood, which is considered as a non-Newtonian fluid. Attention was focused on the effect of the wall elastic property, fluid non-Newtonian property, stenosis percent and tapering angle on stream line distribution, dimensionless WSS, and dimensionless axial velocity profile. The following are the main conclusions drawn from the present investigation.

- For fluid flow inside elastic artery, it can be concluded that:-

a. When the flow rate was increased the artery was expanded, therefore it tends to absorb the incoming as what happens in cases of septic shock for example; vice-versa, the artery was shrined when the flow rate was decreased, thus increasing the actual discharge and its bulk as what happens in cases of hypovolemic shock for example.

b. Expansion of artery diameter leads to wider axial velocity profiles and more blunted in the center.

c. Expansion of artery leads to decrease in the WSS.

d. Expansion of artery leads to a less extended separated region after the stenosis.

- For non-Newtonian model of fluid flow inside elastic artery, it can be concluded that:-

The non-Newtonian model of fluid decreases the WSS distribution. Therefore, elasticity of the wall and non-Newtonian behavior of the blood are key factors affecting the flow characteristics. It's necessary to take into consideration when the relationship between the blood circulation and vascular diseases is investigated.

-For percentage reduction, (0%, 30%, 40% and 50%) stenosis, effects on non-Newtonian model of fluid flow inside elastic artery, it can be concluded that:-

The narrowing blood artery causes an increase in velocity and producing large WSS at the throat of the stenosis. In addition to low shear stress at the distal side of stenosis. It is noticed that the WSS upstream of the stenosis doesn't disturb, whether the stenosis exists or not.

- For tapering angles ($0^{\circ}, 0.1^{\circ}$, and 0.2°) effects on non-Newtonian model of fluid flow inside elastic artery, WSS was increased as tapering angle of artery increased ($0^{\circ}, 0.1^{\circ}$, and 0.2°), due to increase in kinetic energy. As the distance into taper section increased WSS was increased.

REFERENCES

[1] Cavalcanti, S., 1995, *Hemodynamics of an Artery with Mild Stenosis*, J. Biomechanics, Vol. 28, No. 4, pp. 387-399.

[2] Chakravarty, S., and Sen, S., 2008, *Analysis of Pulsatile Blood Flow in Constricted Bifurcated Arteries with Vorticity-Stream Function Approach*, Journal of Medical Engineering & Technology, Vol. 32, No. 1, pp. 10 – 22.

[3] Chaniotis, A.K., Kaiktsis, L., Katritsis, D., Efstathopoulos, E., Pantos, I., and Marmarellis, V., 2010, *Computational Study of Pulsatile Blood Flow in Prototype Vessel Geometries of Coronary Segments*, Physica Medica, Vol. 26, pp. 140-156.

[4] Chen, J., Lu, X., and Wang, W., 2006, *Non-Newtonian Effects of Blood Flow on Hemodynamics in Distal Vascular Graft Anastomoses*, Journal of Biomechanics, Vol. 39, pp.1983–1995.

[5]Devajyoti and Moumita ,2013, *Study of Blood Flow Inside an Inclined Non-Uniform Stenosed Artery*, International Journal of Mathematical Archive-4(5), 33-42.

[6] Fung, Y.C., 1986, *Biomechanics Circulation*, First Edition, Springer-Verlag New York, Inc.

[7] Fung, Y.C., 1997, *Biomechanics Circulation*, Second Edition, Springer-Verlag New York, Inc.

[8] Javadzadegan1, A., Esmaeili, M., Majidi, S., and Fakhimghanbarzadeh, B., 2009, *Pulsatile Flow of Viscous and Viscoelastic Fluids in Constricted Tubes*, Journal of Mechanical Science and Technology, Vol.23, pp.2456-2467.

[9] Johnston, B.M., Johnston, P.R., Corney, S., and Kilpatrick, D., 2006, *Non-Newtonian Blood Flow in Human Right Coronary Arteries: Transient Simulations*, Journal of Biomechanics, Vol. 39, pp. 1116–1128.

[10] Khaled Saad MEKHEIMER, Faiza SALAMA and Mhamod ELKOT3, 2015, *The Unsteady Flow of a Carreau Fluid Through Inclined Catheterized Arteries Having a Balloon with Time-Variant Overlapping Stenosis,* Applied Mathematics ,Walailak J Sci & Tech; 12(10): 863-883.

[11] Liu, G, Wang, X., Ai, B., and Liu, L., 2004, *Numerical Study of Pulsating Flow through a Tapered Artery with Stenosis*, Chinese Journal of Physics, Vol. 42, No. 4-I, pp.401-409.

[12] Mandal, P.K., (2005), *An Unsteady Analysis of Non-Newtonian Blood Flow through Tapered Arteries with a Stenosis*, International Journal of Non-Linear Mechanics, Vol.40, pp.151-164.

[13] Mandal, P.K., Chakravarty, S., Mandal, A., and Amin, N., 2007, *Effect of Body Acceleration on Unsteady Pulsatile Flow of Non-Newtonian Fluid through a Stenosed Artery*, Applied Mathematics and Computation, Vol. 189, pp. 766–779.

[14] Misra, J.C., and Shit, G.C., 2007, *Effect of Magnetic Field on Blood Flow through an Artery: a Numerical Model*, Вычислительные технологии, Том. 12, No. 4.

[15] Moayeri, M.S., and Zendehbudi, G.R., 2003, *Effects of Elastic Property of the Wall on Flow Characteristics through Arterial Stenoses*, Journal of Biomechanics, Vol. 36, pp. 525– 535.

[16] Nguyen, K.T., Clark, C.D., Chancellor, T.J., and Papavassiliou, D.V., (2008), "Carotid Geometry Effects on Blood Flow and on Risk for Vascular Disease", Journal of Biomechanics, Vol. 41, pp.11-19.

[17] Pedrizzetti, G., Domenichini, F., Tortoriello, A., and Zovatto, L., 2002, *Pulsatile Flow Inside Moderately Elastic Arteries, Its Modelling and Effects of Elasticity*, Computer Methods in Biomechanics and Biomedical Engineering, Vol. 5, No. 3, pp. 219–231.

[18] Pontrelli, G., 1999, *Blood Flow through an Axisymmetric Stenosis*, Istituto per le Applicazioni del Calcolo – CNR, Viale del Policlinico, 137, 00161 Roma, Italy.

[19] Siouffi, M., Deplano, V., and Pelissier, R., 1998 *Analysis of Unsteady Flows through a Stenosis*, Journal of Biomechanics, Vol. 31, pp.11-19. , Experimental

[20] Syeda Reham Shahed, Mohammad Ali and Md. Quamrul Islam 2013, *Numerical Analysis of Hemodynamic Forces Through Stenotic Artery*, Journal of Mechanical Engineering, Vol. ME 43, No. 1, Transaction of the Mech. Eng. Div., The Institution of Engineers, Bangladesh.

[21] Tang, D., Yang, C., Kobayashi, S., Zheng, J., and Vito, R.P., 2003, *Effect of Stenosis Asymmetry on Blood Flow and Artery Compression: A Three-Dimensional Fluid-Structure Interaction Model*, Annals of Biomedical Engineering, Vol. 31, pp.1182-1193.

[22] Titus, P. and Balázs, A. , 2014,*Mathematical Models and Numerical Simulations for The Blood Flow*, Ph.D Thesis, Faculty of Mathematics and Computer Science ,Babe-Bolyai" University, Cluj-Napoca.

[23] Tu, C., and Deville, M., 1996, *Pulsatile Flow of Non-Newtonian Fluids through Arterial Stenoses*, J. Biomechanics, Vol. 29, No. 7, pp. 899-908.